Extending The Waveguide Mesh To Represent Viscous Absorption

NATHAN FRASER† RICHARD HALL§

Dept. Computer Science & Engineering,
La Trobe University, Melbourne,
3086, Victoria, Australia

Abstract: Waveguide mesh models that simulate airborne acoustics currently need additional ad–hoc filters to represent absorption. In this paper we show that computational fluid dynamics, thus viscous absorption, can be included in these models, and describe an empirical investigation into an extended mesh model's ability to represent viscous absorption for acoustics. Applications include audio signal processing and computer generated sound.

Key-Words: Acoustics, 2D Waveguide Mesh, Lattice Boltzmann

1 Introduction

A digital waveguide mesh (DWM) is a finite–difference, time domain computational model that can simulate aspects of airborne acoustic (room) phenomena [1, 2]. Spatial dimensions are discretised into a regular lattice of signal processing elements which are joined by unit delays and are updated synchronously in discrete time steps [3, 4]. Absorption phenomena are not native to DWMs; digital filters can add it both at every node in the lattice to impact every update [5], or to correct output signals. In both cases an audio engineer selects a desired frequency profile then uses curve fitting (a non–physical and non–intuitive mechanism) to tweak the signal to match this profile.

Making absorption native to DWMs requires the addition of relaxation phenomena due to viscous, thermal and molecular losses [6]. For audible acoustics in gases, the viscous and thermal (or classical) losses account for most of the absorption [7]. Furthermore, losses due to fluid viscosity are typically greater than those due to thermal conductivity. A class of physical models which natively encapsulates viscous fluid losses are the Lattice Boltzmann models (LBM) to which DWMs are remarkably similar in design. LBMs use a a regular lattice to solve the Navier–Stokes equations for fluid flow [8] in the macroscopic limit; thus they could simulate acoustics with absorption phenomena [9]. They have already been used to model acoustic wave generation in wind instruments [10], and non–linear acoustics [11].

In this paper, a LBM for simulation of incompressible fluid flow in 2–dimensions is tested for its ability to represent the viscous component of acoustic absorption in a fluid medium. In section 2 we outline the design of the model used. We then describe experiments which investigate the model's ability to represent viscous absorption in section 3. Finally, in section 4 we outline future work and applications of the model.

2 Method

For empirical tests of the LBM, a 2–dimensional lattice with 9 fluid velocities (denoted D2Q9 in Figure 1) was used with a single relaxation time or BGK kinetic approximation [12]. The lattice structure is almost identical to that used for the interpolated rectilinear waveguide mesh [13]. We use a 2–dimensional lattice for two reasons: such approximations are able to represent many audio effects to acceptable accuracy [14, 1]; and they can be warped to account for 3–D effects [15].

Lattice Boltzmann models compose a family of discrete–time discrete–velocity approximations of the Boltzmann equation for fluid flow:

$$\frac{\partial f}{\partial t} + \boldsymbol{v}\nabla f = \Omega(f)$$

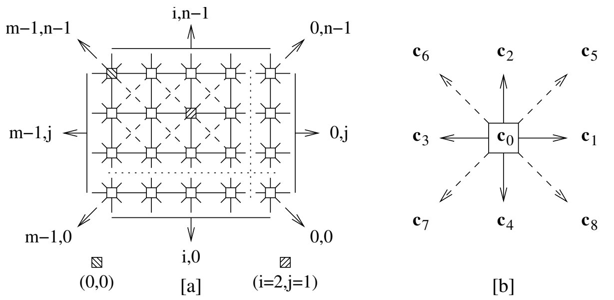

Figure 1: D2Q9 Topology: [a] Nodes are arranged in a 2–dimensional rectilinear lattice of size $m \times n$, with links to nearest (solid) and next–nearest (dashed) neighbours, and periodic boundaries as indicated. [b] Each fluid node has 9 link velocities $\boldsymbol{c}_0 \ldots \boldsymbol{c}_8$ and three lattice speeds: 0, 1 and $\sqrt{2}$.

Where statistical mass distributions f of particles move with velocity $\boldsymbol{v}$ and are redistributed according to a kinetic collision function Ω [16]. Replacing $\boldsymbol{v}$ with a set of discrete velocities, and replacing the collision function Ω with a single relaxation time (τ) kinetic approximation [12] yields a discrete velocity Boltzmann equation [17]:

$$F_i(\boldsymbol{x} + \boldsymbol{c}_i \Delta t, t + \Delta t) - F_i(\boldsymbol{x}, t) = -\frac{1}{\tau}\left(F_i(\boldsymbol{x}, t) - F_i^{(eq)}(\boldsymbol{x}, t)\right) \tag{1}$$

Where the position of a node is denoted by $\boldsymbol{x}$, mass functions F_i represent the quantity of mass at that node moving according to the velocity $\boldsymbol{c}_i$ and equilibrium functions $F_i^{(eq)}$ express the state nodes would relax to, and hence the desired dynamics of the system.

If $1/\tau$ is replaced with ω and Δt is set to 1, the state and evolution of nodes on the lattice with local mass density ρ, local momentum $\boldsymbol{j}$, and local velocity $\boldsymbol{u}$ are described by:

$$\rho(\boldsymbol{x}, t) = \sum_i F_i(\boldsymbol{x}, t) \tag{2}$$

$$\boldsymbol{j}(\boldsymbol{x}, t) = \rho(\boldsymbol{x}, t)\, \boldsymbol{u}(\boldsymbol{x}, t) = \sum_i \boldsymbol{c}_i F_i(\boldsymbol{x}, t) \tag{3}$$

$$F_i(\boldsymbol{x} + \boldsymbol{c}_i, t + 1) = F_i + \omega\left(F_i^{(0)} - F_i\right) \tag{4}$$

The left hand side of (4) represents streaming of mass distributions to adjacent nodes along lattice velocities (see Figure 1), while the right hand side represents relaxation toward an equilibrium state that conserves local mass and momentum. The equilibrium functions $F_i^{(0)}$ chosen for the LBM tested in this paper are formed from a truncated power series of local momentum and mass density for the simulation of a linear and incompressible fluid flow:

$$F_i^{(0)}(\rho, \boldsymbol{j}) = \frac{W_i}{\rho_0}\left\{\rho + \frac{1}{A}\boldsymbol{c}_i \cdot \boldsymbol{j} + \frac{1}{2\rho A}\left[\frac{1}{A}(\boldsymbol{c}_i \cdot \boldsymbol{j})^2 - \boldsymbol{j}^2\right]\right\} \tag{5}$$

Weights W_i and the free parameter A are chosen to maximise stability of the underlying hydrodynamic system for all lattice sizes [18], and to obtain a solution at the macroscopic limit of the Navier–Stokes equations. The values used (as given in [8]) along with the discrete lattice velocities are:

$$\begin{array}{rcll}
\boldsymbol{c}_i & = & (0,0) & i = 0 \\
\boldsymbol{c}_i & = & (\pm 1, 0) & i = 1,3 \\
\boldsymbol{c}_i & = & (0, \pm 1) & i = 2,4 \\
\boldsymbol{c}_i & = & (\pm 1, \pm 1) & i = 5,6,7,8 \\
W_i/\rho_0 & = & \frac{4}{9} & i = 0 \\
W_i/\rho_0 & = & \frac{1}{9} & i = 1,2,3,4 \\
W_i/\rho_0 & = & \frac{1}{36} & i = 5,6,7,8 \\
A & = & \frac{1}{3} &
\end{array} \tag{6}$$

Substituting these values into (5) gives the specific functions:

$$F_i^{(0)} = \begin{cases} \frac{4}{9}\rho\left[1 - \frac{1}{2}\boldsymbol{u}^2\right] & i = 0 \\ \frac{1}{9}\rho\left[1 + 3(\boldsymbol{c}_i \cdot \boldsymbol{u}) + \frac{9}{2}(\boldsymbol{c}_i \cdot \boldsymbol{u})^2 - \frac{1}{2}\boldsymbol{u}^2\right] & i = 1,2,3,4 \\ \frac{1}{36}\rho\left[1 + 3(\boldsymbol{c}_i \cdot \boldsymbol{u}) + \frac{9}{2}(\boldsymbol{c}_i \cdot \boldsymbol{u})^2 - \frac{1}{2}\boldsymbol{u}^2\right] & i = 5,6,7,8 \end{cases} \tag{7}$$

Combining (2), (3), (4) and (7) produces a macroscopic Navier–Stokes approximation with a lattice sound speed of $c_s = 1/\sqrt{3}$. The acoustic pressure (p_a) and kinematic shear viscosity (ν) terms are [8]:

$$p_a(\boldsymbol{x}, t) \simeq (\rho(\boldsymbol{x}, t) - \rho_0)/3 \tag{8}$$

$$\nu = \frac{2 - \omega}{6\omega} \tag{9}$$

Acoustic pressure is approximate since the application of input pressures by a small change in local mass density modifies average mass density, and the pressure is assumed to be proportional to density. ρ_0 is used as an approximation of the average which is correct only at initialisation. So long as input signals contain no DC offset, this approximation provides a valid estimate of acoustic pressure, as the average density on the lattice will remain close to ρ_0.

For our empirical experiments (see Figure 2), an input signal was fed into a chosen lattice geometry and pressure measurements were taken at specific locations on the lattice for a chosen number of update steps. The values for p_a, mass distributions $F_{0\ldots8}$ and a temporary update array $F'_{1\ldots8}$ were stored in a multi–dimensional array. F_i's were initialised from a specified ρ_0 then the steps [a-d] in Figure 3 were repeated. Output waveforms were analysed using the numerical computation package Octave [19] and visualisations were obtained from

RMS pressure plot bitmaps, which were either normalised in amplitude or converted to a visual representation of relative sound pressure level in decibels (dB).

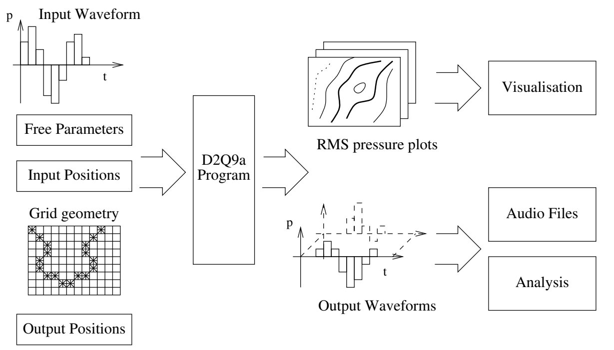

Figure 2: Test environment.

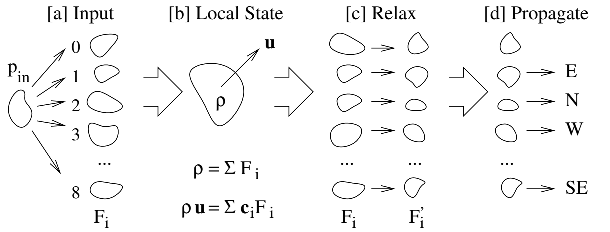

Figure 3: Node update process at each iteration: [a] Input pressure is converted to mass and distributed to the mass functions F_i. [b] Local mass density, velocity and pressure are calculated from the F_i. [c] Equilibrium functions $F_i^{(0)}$ and intermediate mass functions F_i' are computed. [d] F_i' are propagated to F_i at adjacent nodes along direction i (except rest mass F_0).

3 Results

An ideal acoustic model should be stable independent of input signal types, geometry, or control parameters (a la [20]). Digital waveguide meshes are normally stable, irrespective of the frequency and amplitude of the input signal. However, lattice Boltzmann models represent mass distributions, and their stability is dependent on all mass distributions maintaining a positive magnitude. Therefore, the use of a mass–based model for simulations which include viscous absorption adds a stability requirement.

Maintaining stability requires each lattice node to maintain a positive mass density for each fluid velocity, and to relax toward its equilibrium state. Negative values of ω and values over 2.0 are unconditionally unstable [8, 21, 22], but between 0 and 2, stability depends on local fluid velocities, with a maximum stable node velocity of about 1/3 [17]. Since input pressures are translated to a small change in mass, the induced velocity and mass distributions are dependent on the relationship between the relaxation parameter ω, and on the relative magnitudes of ρ_0 and input pressures p_{in}.

To determine usable relative magnitudes of ρ_0 and p_{in}, tests were run on three lattices of size 10x10, 20x20 and 50x50 for values of ω between 0 and 2, and for ratios of p_{in}/ρ_0 ranging from 10 to 0.01. The lattice was stimulated at a single node using a white noise signal, randomly distributed between -1 and 1 and run until instability occurred or to a maximum number of iterations. A white noise signal was used as a worst–case acoustic input, as it has a fairly uniform power distribution across the frequency spectrum.

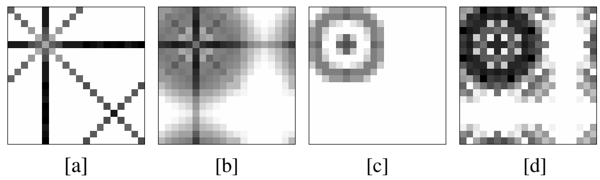

Figure 4: Example wave propagation from stability tests, RMS pressure plots in dB, averaged over 2 iterations 10 steps into the computation. [a] $\omega = 0.0$, [b] $\omega = 0.5$, [c] $\omega = 1.5$, [d] $\omega = 1.99$.

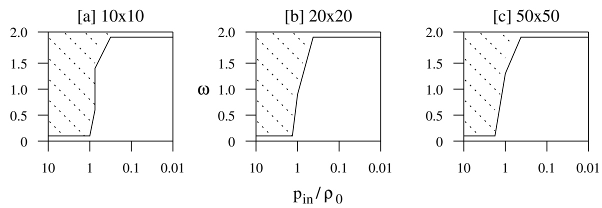

Figure 5: Stable regions of p_{in}/ρ_0 against ω for three mesh sizes: [a] 10x10, [b] 20x20, and [c] 50x50 units. Unstable regions are indicated by dotted lines.

Stable responses were obtained for all tests where ω was 0, however this is a degenerate case where masses travel with a lattice speed of 1 along the primary and diagonal axes away from the input node. No dispersion takes place, as shown in the pressure plot of Figure 4a. At $\omega = 2$, unstable responses were measured for all grid sizes. Results for each

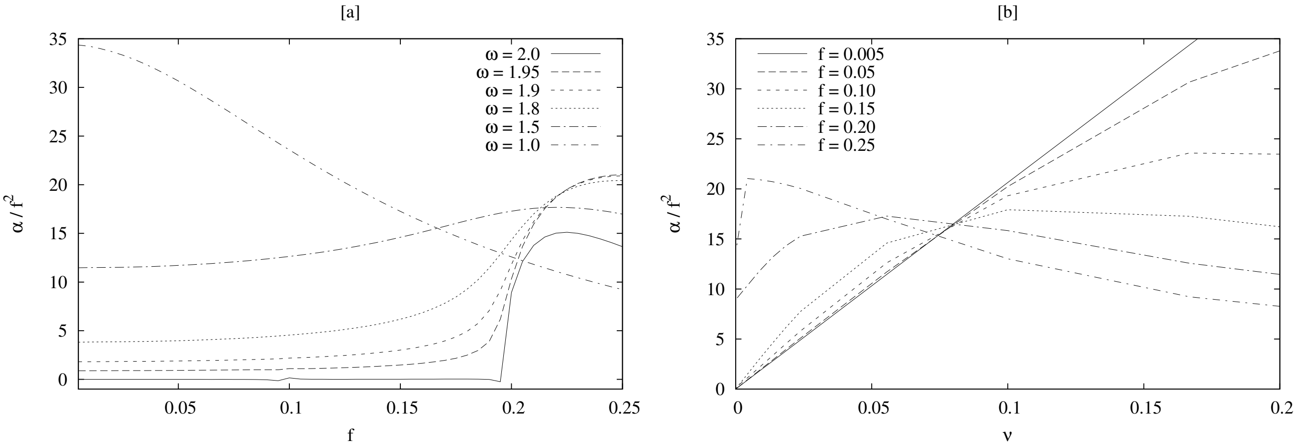

Figure 6: Plots of relative absorption coefficient α/f^2 against [a] frequency f and [b] viscosity ν, measured from attenuation of a single–frequency periodic plane wave propagating freely along a lattice of size 800×40

lattice size are plotted in Figure 5 and show a stable response across the full range of $0 < \omega < 2$ when p_{in}/ρ_0 is of the order 0.1 or less, which is consistent with recommendations in [22]. For low values of ω, less than about 0.8, stable acoustic responses appeared to be over–damped, and contained significant direction–dependent error at short ranges (Figure 4b). Close to $\omega = 2$, wave propagation appeared to become slightly noisy and more direction dependent (Figure 4d). From the measurements taken, D2Q9 is stable for acoustic simulations where the ratio between p_{in} and ρ_0 is approximately 0.1, thus absorption was measured within these bounds.

It is customary to represent absorption by a dimensionless quantity α which represents the spatial rate of decrease in intensity level. This quantity is dependent on both the transmission medium properties and wave frequency. For low (audible) frequencies, it is well approximated by a sum of the three components due to viscous, thermal and molecular losses, with the viscous component (α_S) approximately proportional to the product of shear viscosity and frequency squared [7]:

$$\alpha_S \simeq C f^2 \nu \tag{10}$$

Where C is a constant based on ρ_0 and the speed of sound.

To measure the relationship between α, ω and f in D2Q9, a single–frequency periodic plane wave was induced on a lattice of size 800x40. For values of ω from 0 to 2, and frequencies from 0.005 to 0.25 of the lattice update rate, the model was iterated until it reached a steady state, then RMS pressures were obtained at distances from 1 to 40 nodes away from the source in the direction of wave propagation. Output pressure plots averaged over at least 2 periods of the input signal were analysed and an absorption coefficient was then determined as follows.

For a single frequency, periodic plane wave of amplitude a_0 at $x = 0$, propagating parallel to, and in the positive x direction, its attenuated amplitude a is given by:

$$a(x) = a_0 e^{-\alpha x} \tag{11}$$

By rearranging (11) and substituting measured RMS pressures, an estimate α was obtained for each combination of ω and f. These results are plotted as α/f^2 against frequency f and viscosity ν in Figure 6. The ideal case is a flat horizontal line in [a] and a straight diagonal line in [b].

For values of ω between 1.5 and 2.0, measured values of α were close to the desired profile for frequencies up to almost 0.2 of the lattice update rate. For ω below 1.5, no meaningful results were obtained except at the lowest input frequencies, since high frequency attenuation reduced signals to insignificant values within the area measured. Plots of α/f^2 against viscosity show good agreement to the desired profile for frequencies below about 0.15 and for ν between 0 and 0.1 ($2.0 > \omega > 1.25$).

4 Conclusion

A computational model for fluid flow was applied to the simulation of airborne acoustics, extending the digital waveguide mesh. Results show the model can represent acoustics with a physical identity better than existing waveguide mesh models, over a particular operational frequency range. Absorption due to viscosity is tunable to a limited range, but has a slightly non–physical character which could be avoided by scaling of signals and space.

The model is currently being evaluated in several other ways. We are investigating the response of the model in terms of sound speed, frequency response, and response to various boundary conditions. We are also investigating the scalability of lattice sizes with respect to attempting real–time simulation, and the possibility of replacing fluid flow equilibrium functions with ones tailored to modeling the lossy wave equation.

There are a number of applications of this model. Physically correct acoustic simulation is desired in digital signal processing, audio engineering, sound synthesis and music. It can add realism and immersion to anechoic sounds, and has potential for direct sound synthesis. Small lattice sizes that can be computed in real–time may be used for the synthesis of sounds from non–physical imaginary musical instruments, whose output is still based on physical behaviour. These instruments could be controlled using a graphical interface or optimised from a desired output profile. Such a graphical interface could also allow the model to be used for educational purposes.

Acknowledgement We would like to thank the Department of Computer Science and Computer Engineering at La Trobe University for providing a vacation scholarship for Nathan.

References

[1] Murphy D.T. and Howard D.M. 2–D Digital Waveguide Mesh Topologies in Room Acoustic Modelling. In *Proceedings of the COST G-6 Conference on Digital Audio Effects*. Verona, Italy, Dec. 2000.

[2] Mullen J., Howard D.M., and Murphy D.T. Digital Waveguide Modelling of the Vocal Tract Acoustics. In *Proceedings of the IEEE Workshop on Applications of Signal Processing to Audio and Acoustics*. New Paltz, NY, Oct. 2003.

[3] van Duyne S.A. and Smith III J.O. Physical modeling with the 2-D digital waveguide mesh. In *Proceedings of the International Computer Music Conference*. Tokyo, Japan, sep 1993.

[4] Bilbao S. Wave and Scattering Methods for the Numerical Integration of Partial Differential Equations. Ph.D. thesis, Stanford University, 2001. `http://www-ccrma.stanford.edu/~bilbao/`.

[5] Huopaniemi J., Savioja L., and Karjalainen M. Modeling of reflections and air absorption in acoustical spaces a digital filter design approach. In *IEEE Workshop on Applications of Signal Processing to Audio and Acoustics*, Oct. 1997.

[6] Bass H.E. and Bauer H.J. Atmospheric Absorption of Sound: Analytical Expressions. *Journal of the Acoustical Society of America*, vol. 52(3), 1972, pp. 821–825.

[7] Kinsler L.E., Frey A.R., Coppens A.B., and Sanders J.V. *Fundamentals of Acoustics*. 3rd ed. John Wiley and Sons Inc., 1982.

[8] Wolf-Gladrow D.A. *Lattice-Gas Cellular Automata and Lattice Boltzmann Models, An Introduction*, vol. 1725 of *Lecture Notes in Mathematics*. Springer-Verlag, Berlin, 2000.

[9] Buick J.M., Neal M.A., and Campbell D.M. The Lattice Boltzmann Model and its Application to Acoustics. In *Proceedings of the 17th International Congress on Acoustics*. Rome, Italy, 2001.

[10] Kühnelt H. Simulating the mechanism of sound generation in flutes using the lattice boltzmann method. In *Proceedings of the Stockholm Music Acoustics Conference*. Stockhom, Sweeden, Aug. 2003.

[11] Buick J.M., Greated C.A., and Gilbert J. Lattice Boltzmann BGK simulation of nonlinear sound waves: the development of a shock front. *Journal of Physics A*, vol. 33, 2000, pp. 3917–3928.

[12] Bhatnagar P.L., Gross E.P., and Krook M. A model for collision processes in gases. I. Small amplitude processes in charged and neutral one–component systems. *Physical Review*, vol. 94(3), May 1954, pp. 511–525.

[13] Savioja L. and Välimäki V. Improved discrete–time modeling of multi–dimensional wave propagation using the interpolated digital waveguide mesh. In *Proceedings of IEEE International Conference on Acoustics, Speech, and Signal Processing ICASSP-97*, vol. 1, Apr. 1997.

[14] Murphy D.T. and Howard D.M. Digital waveguide modelling of room acoustics: comparing mesh topologies. In *Proceedings of the 25th EUROMICRO Conference*, vol. 2, Sep. 1999.

[15] Chopard B., Luthi P.O., and Wagen J.F. Lattice Boltzmann method for wave propagation in urban microcells. *IEE Proceedings–Microwaves, Antennas and Propagation*, vol. 144(4), Aug. 1997, pp. 251–255.

[16] Buick J.M. Lattice Boltzmann Methods in Interfacial Wave Modelling. Ph.D. thesis, University of Edinburgh, 1997. `http://www.ph.ed.ac.uk/~jmb/thesis/tot.html`.

[17] Sterling J.D. and Chen S. Stability Analysis of lattice Boltzmann Methods. *Journal of Computational Physics*, vol. 123, 1996, pp. 196–206.

[18] Worthing R.A., Mozer J., and Seeley G. Stability of lattice Boltzmann methods in hydrodynamic regimes. *Physical Review E*, vol. 56(2), 1997, pp. 2243–2253.

[19] Eaton J.W. GNU Octave, a high-level language, primarily intended for numerical computations. `http://www.octave.org/`.

[20] Castagne N. and Cadoz C. 10 Criteria for evaluating physical modelling schemes for music creation. In *Proceedings of the 6th International Conference on Digital Audio Effects*. London, UK, Sep. 2003.

[21] Lallemand P. and Luo L.S. Theory of the lattice Boltzmann method: Dispersion, dissipation, isotropy, Galilean invariance, and stability. *Physical Review E*, vol. 61(6), Jun. 2000, pp. 6546–6562.

[22] Buick J.M., Greated C.A., and Campbell D.M. Lattice BGK Simulations of sound waves. *Europhysics Letters*, vol. 43(3), Aug. 1998, pp. 235–240.